J. Chem. Sci., Vol. 118, No. 1, January 2006, pp. 135–154.

Ionic conduction in the solid state

P PADMA KUMAR and S YASHONATH

Solid State and Structural Chemistry Unit, Indian Institute of Science, Bangalore 560 012
e-mail: yashonat@sscu.iisc.ernet.in

Abstract. Solid state ionic conductors are important from an industrial viewpoint. A variety of such conductors have been found. In order to understand the reasons for high ionic conductivity in these solids, there have been a number of experimental, theoretical and computational studies in the literature. We provide here a survey of these investigations with focus on what is known and elaborate on issues that still remain unresolved. Conductivity depends on a number of factors such as presence of interstitial sites, ion size, temperature, crystal structure etc. We discuss the recent results from atomistic computer simulations on the dependence of conductivity in NASICONs as a function of composition, temperature, phase change and cation among others. A new potential for modelling of NASICON structure that has been proposed is also discussed.

Keywords. Ionic conduction; solid state; atomistic computer simulations; NASICON structure.

1. Introduction

There exist many solids with high ionic conductivity ($>10^{-4}\ \Omega^{-1}\ cm^{-1}$) and they are of immense use in diverse technological applications. Some of these solids which are also good electronic conductors are often referred to as 'mixed conductors', while the term 'superionic conductor' or 'fast ion conductor' is reserved for good ionic conductors with negligible electronic conductivity.[1] One of the most important use of superionic conductors is, as electrolytes in battery applications and hence, often, they are referred to as 'solid electrolytes' as well. There are many advantages in electrochemical devices using solid electrolytes instead of liquid electrolytes. These include, among others, longer life, high energy density, no possibility of leak etc., and are particularly suitable in compact power batteries used in pace-makers, mobile telephones, laptops etc. Mixed ion conductors find application in electrochemical devices as electrode materials.

Here we provide a survey of the literature of the solids with high ionic conductivity. Some of the developments in the past 3–5 years may not be discussed here.

Dedicated to Prof J Gopalakrishnan on his 62nd birthday
*For correspondence

2. A brief history of superionic conductors

The study of ionic conduction in solid state originated way back in 1838 when Faraday discovered that PbF_2 and Ag_2S are good conductors of electricity.[2,3] These solids are, the first ever discovered solid electrolyte and intercalation electrode respectively. The discovery of good Na^+ mobility in glass by Warburg[4] as well as the first transference number measurements by Warburg and Tegetmeier[5] are important contributions in the study of solid ionic conductors. Yttria (Y_2O_3) stabilized zirconia (ZrO_2), after Nernst[6] in 1900, as well as AgI, after Tubandt and Lorenz[7] in 1914, are among the other superionic conductors discovered in the early days. Katayama[8] in 1908 demonstrated that fast ionic conduction can be made use of in potentiometric measurements. Another important discovery is that of the first solid oxide fuel cell by Baur and Preis[9] in 1937 using yttria-stabilized zirconia as the electrolyte. The field of solid electrolytes did not seem to have gained much in the later years until in 1957 Kiukkola and Wagner[10] carried out extensive potentiometric measurements using solid electrolyte based electrochemical sensors.

Silver ion conducting solids, such as Ag_3SI[11] and $RbAg_4I_5$,[12,13] were discovered in the 1960s. The use of Ag_3SI, by Takahashi and Yamamoto,[14] and $RbAg_4I_5$, by Argue and Owens,[15] in electrochemical cells were demonstrated soon after this. There was a burst of enthusiasm following the discovery of high

ion mobility in *b*-alumina ($M_2O.xAl_2O_3$, where M = Li, Na, Ag, K, Rb, NH_4 etc.) by Yao and Kummer in 1967.[16] Na-*b*-alumina was successfully used in Na/S cell by Kummer and Weber.[17] The discovery of *b*-alumina, an excellent solid electrolyte with a fairly rigid framework structure, boosted searches for newer superionic conductors with skeleton structures. This led to the synthesis of gallates, by Kuwabara and Takahashi[18] and Boilot *et al*,[19] and ferrites, by Takahashi *et al*,[20,21] which are *b*-alumina type compounds with the Al replaced by Ga and Fe respectively. Lamellar structures of the kind $K_{0.72}L_{0.72}M_{0.28}O_2$, where L = Se or In and M = Hf, Zr, Sn, and $Na_{0.5}In_{0.5}Zr_{0.5}S_2$ or $Na_{0.8}Zr_{0.2}S_2$ having high electrical conductivities were also synthesized following this.[22,23]

Another advance in the tailored making of superionic solids was when Hong[24] and Goodenough *et al*[25] reported high conductivity in 'skeleton' structures involving polyhedral units. The skeleton structure consists of a rigid (immobile) subarray (sublattice) of ions which render a large number of three-dimensionally connected interstitial sites suitable for long range motion of small monovalent cations.[25] Hong reported synthesis and characterization of $Na_{1+x}Zr_2Si_xP_{3-x}O_{12}$, where $0 \le x \le 3$, now popularly known as NASICONs.[25] It is observed that the best conductor of the series is $Na_3Zr_2Si_2PO_{12}$ ($x = 2$). Its conductivity is comparable to Na-*b*-alumina above 443 K. $Na_3Zr_2Si_2PO_{12}$ is the first reported Na^+ ion conductor with three dimensional conductivity. Hong[24] reported the synthesis and structure of Li, Ag and K counterparts of NASICONs as well. $LiZr_2(PO_4)_3$ is yet another superionic conductor at high temperature. The enormous ionic substitutions possible in $NaZr_2(PO_4)_3$ led to the synthesis of a very large number of compounds which now find applications in diverse fields of materials science.

Goodenough *et al*[25] investigated the possibility of fast ion transport in various other skeleton structures as well. The other skeleton structures examined includes that of the high-pressure-stabilized cubic Im_3 phase of $KSbO_3$ and $NaSbO_3$, defect-pyrochlore structure of the kind AB_2X_6, carnegieite structure of high-temperature $NaAlSiO_4$ as well as the NASICONs.[25] While the $Na_3Zr_2Si_2PO_{12}$ is found to be the best in the series, $NaSbO_3$ is also a promising material for solid electrolyte applications.[25]

Since 1970, a good number of studies focusing on the synthesis and characterization of lithium ion conductors appeared. Search for the lithium ion conductors are motivated by the small ionic radii of Li^+, its lower weight, ease of handling and its potential use in high energy density batteries. Li_2SiO_4 is one of the earliest superionic solids known.[26] Li_2SiO_4 as well as many solid solutions involving it shows high ionic conductivity and has been the subject of many interesting studies.[27–29] Li_2SiO_4[30] as well as its non-stoichiometric solid solution $Li_{4-3x}Al_3SiO_4$ ($0 \le x \le 0{\cdot}5$)[31] are promising Li superionic conductors. Some of the important Li ion conductors that have attracted investigations are Li_3N,[32,33] Li-*b*-alumina,[34] NASICON type, $LiZr_2(PO_4)_3$,[35] $LiHf_2P_3O_{12}$[35] etc., ternary chalcogenides like $LiInS_2$,[36] $Li_4B_7O_{12}X$ (X = Br, Cl or S).[37]

While most of the superionic conductors discussed above are crystalline, many glassy[38–40] as well as polymer[41–44] electrolytes are also being studied extensively.

3. Conduction mechanisms

For ionic conductivity, transport of one or more types of ions across the material is necessary. In an ideal crystal all constituent ions are arranged in regular periodic fashion and are often stacked in a close-packed form. Thus there is little space for an ion to diffuse. Often, the available space is just enough for vibration around its equilibrium position. However, at any non-zero temperature there exist defects. These could, for example, be positional disorder due to deviation from ideal stacking. The degree of such disorder can vary from one material to another or even from one temperature or pressure to another in the same material. At zero temperature the free energy is dominated by the potential energy. Hence the arrangement of ions in an ideal crystal at zero temperature is such that the total potential energy of the system is the lowest. As the temperature of the system increases, the contributions to free energy from entropy becomes more and more prominent. The entropy, as it is often described, is a measure of the degree of disorder. Thus the origin of the crystal defect arises from the system attempting to minimize the free energy through an increase in the entropy.

Two types of defects important in the context of ion mobility in crystals are 'Schottky' and 'Frenkel' defect. These belong to the class of 'point defects' in crystals. Schottky defect refers to the crystal imperfection in which a pair of ions, one cation and the other an anion, disappears leaving their positions

vacant. A single ion missing from its regular position and wandering in interstitial sites results in Frenkel defect. Interstitial sites have different environments, in terms of the number or type of their neighbours or its separation from the neighbours, than the regular sites. Interstitial sites, or simply interstitials, are not energetically favourable for ions; their occupancy, though, is driven by entropy enhancement discussed earlier. Both Frenkel and Schottky defects result in vacant sites in the crystal and any ion in the immediate vicinity can jump to one of the vacant sites. This leaves the previous site of the ion vacant which could now host another ion. This process can lead to transport of ions across the solid giving rise to conductivity. This mechanism is termed *vacancy migration*. NaCl is a typical example wherein the ionic conduction is through vacancy migration. The ion that moves to the interstitial site, giving rise to a Frenkel defect, can subsequently jump to a neighbouring interstitial site and so on, resulting in long distance motion of the ion. This mechanism is referred to as *interstitial migration*. Apart from these two mechanisms, there is yet another mechanism called *interstitialcy mechanism*. This refers to the conduction mechanism through cooperative movement of two or more ions. In crystals where this mechanism is known to operate, the occupancies of the sites as well as the interstitials are such that for an ion to jump to a neighbouring site or interstitial requires one or more neighbouring ions to be pushed elsewhere. This is believed to be the conduction mechanism in Na-*b*-alumina.

4. Classification of ionic conductors

Presence of disorder or defects are necessary for ionic transport in a solid. We have discussed in the previous section how point defects in a crystal can lead to transport of ions. The density of defects, which is the number of defects per unit volume, in a crystal depends considerably on various factors like, the structure, the temperature, the presence of impurity ions, the nature of chemical bonding between constituent ions etc. Thus classification of ionic solids (not necessarily superionic conductors) are proposed based on the type of defect or disorder responsible for ionic conduction. One useful classification of crystalline ionic conductors by Rice and Roth[1,47] is as follows:

Type I: These are ionic solids with low concentration of defects $\sim 10^{18}$ cm^{-3} at room temperature. These are generally poor ionic conductors like, NaCl, KCl etc.

Type II: Ionic solids with high concentration of defects, typically, $\sim 10^{20}$ cm^{-3} at room temperature belong to this category. These are generally good ionic conductors at room temperature and, often, fast ion conductors at high temperatures. Stabilized ZrO_2, CaF_2 etc. are examples.

The conduction mechanism in type I and II conductors is 'vacancy migration'.

Type III: Best superionic conductors like Na-*b*-alumina, $RbAg_4I_5$ etc. belong to this class of compounds. These solids have a 'molten' sub-lattice or 'liquid like' structure of the mobile ions whose concentration is typically 10^{22} cm^{-3}. In other words at least one type of ions constituting the crystal are highly delocalized over the sites available to them. The free energy associated with the regular sites and interstitial sites, in these solids, are very similar and hence they are almost equally favourable for occupancy of ions. The conduction mechanism in such solids are mostly 'interstitial' or 'interstitialcy migration' or a mix of both.

5. Ionic conductivity

As is evident from the previous discussions the factors that influence the conductivity in the solid state are the concentration of charge carriers, temperature of the crystal, the availability of vacant-accessible sites which is controlled by the density of defects in the crystal and the ease with which an ion can jump to another site etc. The last of the above discussed factors, namely, the ease with which an ion can jump to a neighbouring site is controlled by the *activation energy*. The 'activation energy' is a phenomenological quantity. It may be said to indicate the free energy barrier an ion has to overcome for a successful jump between the sites. Among the various factors that influence the ionic conductivity of a crystal the activation energy is of utmost importance since the dependence is exponential. It can be measured quiet conveniently by experiments. The activation energies are most commonly deduced using the Arrhenius expression, given by,

$$s = (A/T)\exp(-E_a/K_BT) \quad (1)$$

where s is the conductivity at temperature T in K, k_B is the Boltzmann's constant, E_a is the activation energy and A is called the pre-exponential factor. The pre-exponential factor, A, contains all the remaining

factors, i.e., other than the activation energy, that influence the ionic conductivity. The activation energy, E_a, may be deduced easily from the slope of the $\ln_e(sT)$ versus T^{-1} plot. The random walk theory support the above functional form of s and also describes A in terms of other factors that influence the ionic conduction.[2]

The Nernst–Einstein expression relates the ionic conductivity to the diffusion coefficient of ions and is particularly useful in molecular dynamics study. The Nernst–Einstein expression suggest that the conductivity,

$$s = nq^2D/k_BT \tag{2}$$

where n is the number of ions per unit volume, q is its charge and D the self-diffusion coefficient of ions,

$$D = zNc(1 - c)a_l^2n/k_BT, \tag{3}$$

where z is the number of nearest neighbour sites of density N, c is the concentration of ions, a_l the distance between the sites and n is the jump frequency given by,

$$n = n_0\exp(-E_a/k_BT), \tag{4}$$

where E_a is the free energy barrier associated with the ion hop between two sites and n_0 is the cage frequency (site frequency) of the ion. The expression suggest that for high diffusivity in solids,

(1) high density of mobile ions (c),
(2) the availability of vacant sites (that can be accessed by the mobile ions) $(1 - c)$,
(3) good connectivity among the sites (requiring conduction channels with low free energy (E_a) barriers between the sites).

5.1 *Common current carrying ions in superionic solids*

Both cations and anions can be carriers of electric current in ionic solids. In general cations have smaller ionic radii than anions and going by the simple logic that 'smaller ions diffuse faster' (though there are situations where this logic does not work – one such situation is the Levitation Effect[?]) one expects cations to diffuse faster in solids. Hence the majority of superionic solids discovered are cation conductors. The current carrying cations commonly found in superionic conductors are Li^+, Na^+, K^+, Ag^+ and Cu^+. This is, of course, disregarding the good proton (H^+) conductors. There are a large number of excellent proton conductors which find immense industrial applications, for example, in fuel cells. The study of proton conductors is regarded as separate field because, often, it is suggested that the basic mechanism of proton transport in systems is quite different from other superionic conductors and one requires to invoke quantum mechanical concepts to explain them.

There are superionic conductors where the charge carriers are anions. However, the list of anion-conducting superionic solids is comparatively small and, so far, among the numerous anions only F^- and O^{2-} are found to be good carriers of electricity. As described above ionic radii or size of the ion is an important factor in deciding the diffusivity of ions and the existence of F^- and O^{2-}-conducting superionic solids is owing to their small ionic radii of 1·36 and 1·21 Å respectively, which falls in between the ionic radii of Na^+ and K^+.

Another factor that influences the diffusivity of ion is the magnitude of the charge it carries. When the charge on an ion is large it is likely to be confined to its site by stronger Coulombic attraction of its neighbouring ions (which are of opposite charge). Also, when the charge on the ions is larger it finds higher activation energy barrier in its jump between sites. This is the reason why the predominant current carrying or conducting species in known superionic solids are monovalent with the exception of oxygen (O^{2-}) which is divalent. It is also noteworthy in this context that most O^{2-}-conductors are superionic only at high temperatures.

6. Experimental probes to study superionic conductors

Various experimental techniques have been employed in the past to study superionic solids. Often, depending on the nature of the system studied, some techniques prove more useful than others. Aspects of primary importance in the study of superionic conductors along with the most common experimental tools employed for the purpose will be briefly discussed below.

6.1 *Structural characterization*

In the previous discussion we saw that long range motions of ions that lead to high conductivity in

these solids require high density of mobile-ion-sites along with a network of 'smooth' conduction channels connecting them. This suggests that there is a close interplay of the structure and conductivity in superionic solids. Hence detailed understanding of the structural features is of particular importance in the context of superionic conductors. As in the case of other crystalline solids, *X-ray* and *neutron diffraction* techniques are commonly employed to elucidate the structure features of superionic solids. Superionic conduction being a bulk property rather than a surface property, optical, electron, scanning tunneling as well as atomic force microscopy are of limited application in characterizing the structure of superionic solids. A preliminary analysis of structure includes the symmetry of the unit cell, the positions of immobile ions as well as the distribution of vacant and occupied mobile-ion-sites in the unit cell. A knowledge of the conduction channels as well as the bottlenecks to ionic motion are other aspects of considerable importance in superionic solids.

6.2 *Thermodynamic properties*

Differential scanning calorimetry (DSC) as well as *differential thermal analysis* (DTA) are useful in deducing the thermodynamical properties of solids. These techniques are particularly important in superionic solids to locate as well as classify structural phase transitions which are observed in most superionic solids. These phase transitions are often associated with a few orders of magnitude changes in conductivity. Hence these transitions are some times referred to as *normal–superionic* transition. In superionic solids, where such structural phase transitions are observed, the enhancement in conductivity is often attributed to the changes in structural features of the solid. Structural phase transitions observed in some superionic solids will be discussed later in this section. Transition temperatures are fairly accurately determined by either of the two techniques mentioned above while the microscopic information regarding the changes in the structural features is deduced from X-ray or neutron diffraction experiments carried out above and below the transition point.

6.3 *Vibrational spectra*

Vibrational spectra of the solids have been recorded using *infrared* (IR), *far-infrared* (FIR) or *Raman*. These techniques are also useful in characterizing superionic solids. The frequencies associated with the diffusive modes of the mobile ions are lower, a few tens in units of cm^{-1}, which is expected. The far-infrared measurements are particularly useful in deducing these low vibrational frequencies of mobile ions. As mentioned above, most superionic solids exhibit structural phase transitions and vibrational spectra can provide valuable insights to the 'mode softening' (which refers to the disappearance of a particular vibrational mode) phenomena associated with structural phase transitions. In some systems it is seen that the vibrational modes of the immobile species also significantly influence the dynamics and transport of the diffusing species. Spectroscopic studies can provide valuable insights into such phenomenon.

6.4 *Conductivity, diffusion coefficient and ion transport*

The net conductivity of a solid has contributions from electrons as well as ions. The *transference number measurements*[1] can be performed to find out the actual charge carriers in a solid. There are many sources of error in conductivity measurements which are to be eliminated before results can be interpreted. The contact resistance and polarization effects at the superionic solid-electrode interface as well as the grain boundary conduction are the predominant among them. *a.c.* impedance measurement (to avoid errors due to polarization effect) using 'four-probe' technique (to avoid errors due to contact resistance) is used to minimize errors due to the first two sources. The conductivity measured at various frequency values of the external field at a given temperature is then extrapolated to zero frequency value to get the *d.c.* conductivity value. The errors due to grain boundary conduction depends on the material as well as the method of preparation, heat treatment etc. The use of single crystals for conductivity measurements is the only solution to this problem. The conductivity measurements are generally performed over a range of temperatures so that activation energies can be calculated (as described in §5). These activation energies can give a rough estimate of the microscopic activation energy barrier encountered by the ion.

As described by the Nernst–Einstein (3) the diffusion coefficient can be deduced from conductivity value. But there are ways, such as the *tracer diffu-*

sion experiment,[46] to estimate the diffusion coefficient directly from experiments. The value of diffusion coefficient measured by tracer diffusion and that deduced from conductivity (using (3)) are in some cases different. The ratio of the two,

$$H_R = D_{Tr}/D_s, \tag{5}$$

where D_{Tr} is the tracer diffusion coefficient and D_s is the diffusion coefficient from Nernst-Einstein relation), is referred to as the 'Haven ratio'. This measures the extent of ion–ion correlation in the superionic solid considered.

6.5 *Microscopic ion dynamics*

Nuclear magnetic resonance (NMR) is a useful experimental probe in gaining insights to the microscopic ion dynamics. Different peaks in the NMR spectrum from a superionic solid can be correlated with different environments of the probing ion (e.g., in Li-NMR it is the different Li environments in the sample that the signals characterize). This helps to identify how many different mobile-ion-sites are being occupied as every site has a different environment. The full width at half maximum (FWHM), which is commonly referred to as the 'line width', of NMR peaks reduces as the mobility of the probed species increases. This is usually called the 'motional narrowing'. This property is quite conveniently made use of in the study of superionic solids to locate the normal–superionic transition. Approximate estimate of activation energies as well as relaxation times of mobile ions can also be obtained from NMR studies.

Quasi elastic neutron scattering (QENS) technique is powerful in depicting the ionic motion in superionic solids, even though they are tedious to perform. The technique has the advantage that ion dynamics can be probed at spatial as well as temporal domains. There are different models of diffusion of ions proposed, such as, *simple diffusion, jump diffusion* and *local motion plus jump diffusion*. QENS results can be analysed to find out which of these diffusion models is appropriate for the superionic conductor under study. The method can also be used to estimate the long time diffusion coefficient values from the behaviour in the limit of small *k*.

While these are the more common experimental techniques used in the study of superionic solids other techniques such as, thermoelectric power measurements,[1] birefringence measurements,[1,47] Hall effect,[1,48,49] surface ion spectroscopy[1,50] etc. have also been used.

Apart from the various experimental techniques discussed above, computer simulation techniques have also been employed in the study of superionic conductors. Considering the relevance of this technique in the present context of the thesis, a description of the same is given.

7. Computer simulation techniques

Computer simulation is a relatively newer technique to study properties of matter. Proposed in the fifties by Metropolis and coworkers, the technique has constantly been improved by various researchers. The field of computer simulation has gained considerably in the recent years from the availability of faster computers and computer simulation has now grown into a power tool and is widely employed in many diverse areas of condensed matter. The unique feature of the technique is the ease with which microscopic, or more appropriately 'nanoscopic', mechanism governing the phenomenon under study can be elucidated. This is indeed the motivation behind employing simulation techniques to the study of superionic solids.

In the following sections we discuss a few of the important simulation techniques used in the study of superionic solids.

7.1 *Monte Carlo*

The Monte Calro (MC) technique originated from the basic idea of von Neumann and Ulam to employ stochastic sampling experiments to solve certain mathematical problems.[51] The technique in its present form was proposed by Metropolis and coworkers in 1953.[52] The name 'Monte Carlo' derives from the extensive use of random numbers.

Statistical mechanics suggest that average of any property, *A*, of the system (can be a system of particles, spins etc.), can be calculated in the canonical (NVT) ensemble as,[53]

$$\langle A\rangle = \frac{\int A(t)\exp(-b\mathbf{H}(t))\mathrm{d}t}{\int \exp(-b\mathbf{H}(t))\mathrm{d}t}, \tag{6}$$

where $\mathbf{H}$ is the Hamiltonian of the system, $b = 1/k_BT$ and t represents all the phase space variables (for

example, all the spatial (x, y, z), as well as momenta (p_x, p_y, p_z) in the case of a system of particles). The Hamiltonian, $\mathbf{H}(t)$, can be split into potential, $\mathbf{U}(r)$ (which depends only on the spatial coordinates), and kinetic, $\mathbf{K}(p)$ (which depends only of the momenta), parts as,

$$\mathbf{H} = \mathbf{K} + \mathbf{U}, \tag{7}$$

The potential function, $\mathbf{U}(r)$, captures all the characteristics of the system and can be quite complex. Later in this section we discuss the intermolecular potentials. The kinetic energy term, $\mathbf{K}$ has the simple functional form, $\mathbf{K} = \sum p_i^2/2m_i$, and hence its contribution to (6) can be evaluated quite easily. Hence, often, (6) is written with $\mathbf{U}(r)$ replacing $\mathbf{H}(t)$.

In order to evaluate the integral in (6) exactly, the entire phase space (in practice, only the configurational space) has to be scanned. For any system of 'reasonable' size, the integration has to be performed over a very large number of variables, which is beyond the power of even the modern computers. The solution to this problem is to perform *importance sampling* suggested by Metropolis and co-workers.[52] Basically, Metropolis's idea was to sample only those regions of the phase space which contribute to the integral in (6). In other wards, those phase space points (configurations) for which the Boltzmann factor (Boltzmann probability),

$$P(t) = \frac{\exp(-b\mathbf{H}(t))}{\int \exp(-b\mathbf{H}(t))\mathrm{d}t} \tag{8}$$

is significant, need be sampled. It may be remembered that for a system at equilibrium, the distribution of configurations correspond to the Boltzmann probability, (8).

Now, if M points are sampled from the distribution $P(t)$, then the average of A may be computed as,

$$\bar{A} = \frac{1}{M}\sum_{i=1}^{M} A(t_i). \tag{9}$$

For large enough M values $\bar{A} \approx \langle A \rangle$, the desired thermodynamic average. But the configurations, t_i's, at which $P(t)$ is significant are not known *a priori*. However, it is possible to construct a 'Markov chain' of configurations, t_1, t_2,…t_i, that approach the desired distribution, $P(t)$, asymptotically.[52] Thus for large enough i, t_i as well as the successive configurations generated, t_{i+1}, t_{i+2} etc. belong to $P(t)$. It is shown[52] that the Markov chain of configurations can be constructed, each from the preceeding one, with the probability of transition ('transition probability') from state j and $j + 1$, defined as,

$$T_{j \to j+1} = \min\{1, \exp(b\Delta\mathbf{U})\}, \tag{10}$$

where $\Delta\mathbf{U} = \mathbf{U}_j - \mathbf{U}_{j+1}$. $\mathbf{U}_j$ and $\mathbf{U}_{j+1}$ are potential energies corresponding to configurations j and $j + 1$, respectively.

The simplest Monte Carlo simulation, in the canonical ensemble, employing the *importance sampling* algorithm, involves the following steps,[54,55]

(1) a configuration, t_1, is chosen and its potential energy, $\mathbf{U}(t_1)$, is evaluated;
(2) another configuration, t_2, is constructed through random displacement where again the energy, $\mathbf{U}(t_2)$ is evaluated;
(3) the quantity, $r_{12} = \exp[b(\mathbf{U}(t_1) - \mathbf{U}(t_2))]$ is then compared with a random number in the interval (0, 1);
(4) the move is said to be 'accepted' and $A(t_2)$ is considered for averaging if and only if r_{12} is greater than or equal to the random number generated. In this case the next configuration, t_3, is generated from t_2 as in step 2;
(5) if r_{12} is smaller than the random number, the move is said to be 'rejected', $A(t_1)$ is considered for averaging instead of $A(t_2)$ and t_3 is generated from t_1 as in step 2.

This procedure is performed iteratively a sufficiently large number of times until satisfactory convergence in $\langle A \rangle$ is obtained. Here it may be noted that the $\langle A \rangle$ is only a simple average over the 'accepted' moves and not the weighted average as in (6). This is because the Boltzmann factor is already taken care of in choosing 'samples' used in averaging. Here it may be noted that the choice of the starting configuration (that corresponds to t_1) is very important. In practice, to avoid the influence of the starting configuration, a few thousand MC steps (an MC step involves performance of all the five points listed above) are excluded from the calculation of averages. The method assumes that the system is *ergodic*, which means every point in its phase space is reachable from any other point without getting 'latched up' in any region of phase space. By introducing some changes in the above algorithm, Monte Carlo technique can be employed to ensembles such

as, constant NPT ensemble,[55,56] isostress-isothermal (constant NPT with variable shape and size simulation cell),[57–59] grand-canonical (μVT) ensemble.[60,61]

7.2 *Molecular dynamics*

The first molecular dynamics (MD) simulation was performed on hard spheres in the late fifties by Alder and Wainwright.[62,63] Later, Rahman[64] carried out successful simulations with a more realistic intermolecular potential, namely, the Lennard–Jones potential. The potentials used are 'conservative'. The calculation involves calculations in the microcanonical ensemble. The Hamilton's equations of motion can be written in Cartesian reference frame as,[65]

$$\dot{\mathbf{r}}_i = \mathbf{p}_i / m, \tag{11}$$

$$\dot{\mathbf{p}}_i = -\nabla_{\mathbf{r}_i}\mathbf{U}(\mathbf{r}_i) = \mathbf{f}_i, \text{ for all, } i = 1, 2,\ldots N, \tag{12}$$

where $\mathbf{r}_i$ is the position and $\mathbf{p}_i$ is the momentum of the ith particle. N is the total number of particles in the system. The molecular dynamics method involves solution of the coupled differential equations (11) and (12). This gives the time evolution of positions and momenta of particles according to equations of motion.

The calculation involves the following steps:

(1) Choose an initial set of positions and velocities for all the particles and calculate forces on each of the ions, $\mathbf{f}_i$, using (12);
(2) from the forces, the accelerations are obtained and with the help of an appropriate integration time step, dt, the velocities (after time dt) of each of the particles can be updated;
(3) from the updated velocities the new positions of the particles (after time dt) are deduced. Any property of interest, which is a function of the positions and velocities of particles, are then calculated.

These three steps constitute the simplest MD step. The MD steps are then repeated and in every step the system advances by a time of dt. So by repeating the cycle, say L times, the system has evolved through $L \times dt$. While the MD calculation discussed above is in the micro-canonical ensemble, variants of this basic algorithm have been developed to carry out simulations in other ensembles, like, isothermal (NVT) ensemble,[57,66–68] isothermal-isobaric (NPT) ensemble,[57,69] isostress-isobaric ensemble (constant NPT with variable shape and size simulation cell).[58,59] One major advantage of MD over the Monte Carlo is the availability of the actual time scale of the processes.

Apart from molecular dynamics and Monte Carlo simulation techniques, briefly discussed above, there are other simulation techniques, like, Langevin dynamics (LD),[70] bond valence equation (BVE)[71] etc., which are essentially classical simulation techniques, and *ab initio* simulation techniques such as density functional theory (DFT),[72] Car–Parrinello molecular dynamics[73] (CPMD), path integral techniques (PIMC)[72–76] etc. These have also been employed in the study of superionic conductors.

8. Intermolecular potentials

As is evident from the above discussions as well as from (6), (7) and (12), the knowledge of interparticle potential is essential to carry out molecular dynamics and Monte Carlo simulations. The potential between particles depends on the spatial electronic distribution around their nuclei. The electrons in the system require quantum mechanical description and hence their dynamics is disregarded. Classical MC and MD simulations, discussed above, deal with dynamics of particles that are describable using Newton's Laws of motion, which include atoms, ions or molecules. Frequently, higher order electrostatic interactions and polarizability interactions are neglected. To compensate for such neglect, the potential parameters between any two given pair of atoms are so adjusted as to reproduce the known experimental properties. Hence, these potentials are effective potentials and the parameters between any pair of atoms often do not reflect the true interactions between them.

8.1 *Lennard–Jones potential*

These potentials represent the simplest of all chemical species namely those that have closed-shell electronic configurations. The rare gas systems are well described by the Lennard–Jones interaction potential given by,

$$\mathbf{U}(r_{ij}) = 4e((s/r_{ij})^{12} - (s/r_{ij})^{6}) \tag{13}$$

where $r_{ij} = |\mathbf{r}_i - \mathbf{r}_j|$, $\mathbf{r}_i$ the position of the ith particle, e and s are parameters whose dimensions are that of energy and length respectively. A choice of e =

120 k_B and s = 3·4 Å is found to be appropriate for simulation studies of Ar. The s is interpreted as the diameter of the atom. It may be noted that at short ranges the potential is repulsive while at long ranges it is attractive. This aspect is an essential feature of all interparticle potentials. The long range attractive part of (13), $-4e(s/r_{ij})^6$, arises due to the 'dispersion' interactions and this functional form is supported by rigorous mathematical derivations. The short range repulsive part, $4e(s/r_{ij})^{12}$, arises due to the strong 'overlap-repulsion' of the electronic clouds. Theoretical, it can be shown that the correct functional form of the repulsive interactions is exponential and not r^{-12}. However, the latter is used to decrease the computational effort involved.

8.2 *Born–Mayer–Huggins potential*

For ionic solids, where the Coulombic interactions dominate, the Lennard–Jones potential is inadequate. One most popularly used in the simulation of ionic systems, particularly alkali halides, is the Born–Mayer–Huggins (BMH) or Tosi and Fumi potential,[77,78] given by,

$$\mathbf{U}(r_{ij}) = \frac{q_i q_j}{r_{ij}} + A_{ij}\exp(-r_{ij}/r_{ij}) - \frac{C_{ij}}{r_{ij}^6} - \frac{D_{ij}}{r_{ij}^8} \qquad (14)$$

where q_i is the charge on the ith ion, A_{ij}, C_{ij} and D_{ij} are respectively the 'over-lap repulsive' energy, dipole–dipole, dipole–quadrupole dispersion energy between the ion pairs i and j. For systems with covalent interactions, 'partial' or 'fractional' charges are used in the BMH potential instead of 'full' charges. The 'full' charge on an ion refers to $Q|e|$, where e is the electronic charge and Q is the oxidation state of the ion. The term involving r_{ij}^{-8} is not very important and often discarded – the resulting functional form is called Born–Mayer (BM) potential. The BM potential with suitable parameters has been successful in simulating a wide range of inorganic solids and their molten phases.[79–83] Simulation studies on superionic solids like, $SrCl_2$,[84] b-alumina,[85–88] Li_3N,[89,90] $Gd_2Zr_2O_7$,[91] $LiMn_2O_4$,[92] ABO_3-type perovskites (where A = La, Ba, Ca, Sr and B = Mn, Co, Ga, Y, Ce, Zr)[93] etc. have also employed BM potential.

8.3 *Vashishta–Rahman potential*

Vashishta and Rahman[94] employed a potential of the kind,

$$\mathbf{U}(r_{ij}) = \frac{q_i q_j}{r_{ij}} + \frac{A_{ij}(s_i + s_j)^{n_{ij}}}{r_{ij}^{n_{ij}}} - \frac{(a_i q_j^2 + a_j q_j^2)}{2r_{ij}^4} - \frac{C_{ij}}{r_{ij}^6}, \qquad (15)$$

in the simulation of AgI, a superionic conductor. Here a_i is the polarizability and s_i is the ionic radii of the ith ion. n_{ij} is an integer between 7 and 11 depending on the charge of the ion pairs i and j. Other parameters of the potential have the same meaning as in (14). This potential was later shown to be quite successful in describing many superionic conductors, like, AgI[94,95] and Ag_2S.[96]

A good number of superionic solids of diverse structural features and thermodynamic behaviours have now been studied by computer simulation techniques.[97–99] In the next section we review some of the important superionic solids investigated by means of computer simulation.

9. Simulation studies on superionic solids

Ratner and Nitzan[100] have classified crystalline superionic solids into 'soft framework materials' and 'covalent framework materials' based on the structural rigidity of the immobile sublattice. This is a useful classification and will be followed in the ongoing discussion.

9.1 *Soft framework solids*

These are 'soft' crystals with low Debye temperature and low cage vibrational frequencies. The interaction among the ions are predominantly ionic and hence show lower melting points in comparison with covalently bonded crystals. The basic 'framework' (the sublattice of the immobile ions) of this class of superionic solids are generally simple as the basic structural moieties are ions. AgI, Ag_2Se, Ag_2S, CaF_2 are examples of superionic solids with soft framework. Most soft framework superionic conductors show sharp $a \leftrightarrow b$ (normal to superionic) transition with a sudden increase in the conductivity.

9.1a *CaF_2-type:* CaF_2 and PbF_2 are among the fairly well-studied fluoride ion conductors.[1,101–104] Both stabilize in *fluorite* structure where the Ca^{+2}/Pb^{+2} forms an fcc lattice and the F^- ions occupies the octahedral sites. The first ever atomistic simulation study on superionic solids is by Rahman[105] on CaF_2. The study made use of the potential suggested by

Kim and Gorden.[106] An interesting aspect of the study is that the octahedral sites, which are completely filled by F^- ions at low temperatures, are underoccupied (with occupancy nearly half) at high temperature (~1600°C). This suggests that there is yet another F^- ion site (other than the usual octahedral sites in the fluorite structure). The structure factor, $F_s(k, t)$, calculated for the F^- ions are found to exhibit two characteristic times, probably, corresponding to the relaxation of F^- ions at these two sites. Later Jacucci and Rahman[107] as well as Dixon and Gillan[7,108,109] extended the work to gain further insights to the ion dynamics in these CaF_2. An interesting observation by Gillan and Dixon[84,97] in CaF_2 is that the site-site jumps of F^- ions are correlated and not independent of one another. More recently, Montani[110] has carried out Monte Carlo investigations of the normal to superionic transition of CaF_2.

Interesting simulation studies exists on other fluoride ion conductors like PbF_2[111] and $SrCl_2$[84,108] etc. The F^- ion diffusion in PbF_2 has been well demonstrated[97,111] to be through occasional jumps between regular sites where they execute vibrational motion for almost all the time.[97,111] The majority of jumps are found to be between nearest neighbour sites while a small fraction of jumps are between the next-neighbour sites. The 'framework' ions in all these (CaF_2, PbF_2 and $SrCl_2$) systems, as expected, are found to be localized executing vibrational motion in their regular sites. More recently Castiglione *et al*[112] have carried out extensive MD simulation on α-PbF_2. The detailed site-hopping analysis carried out[112] suggest vacancy-promoted ionic motion in α-PbF_2.

9.1b *AgI-type:* The low-temperature phase of AgI (β-AgI) has wurtzite structure with the iodines arranged in an *hcp* lattice. The β phase transforms to the α phase, reversibly, at around 420 K. The ionic conductivity shows a sudden jump of about three orders of magnitude at the transition point.[1,113] In α-AgI (the high-temperature-superionic phase) the iodine forms a bcc lattice and the Ag^+ are highly disordered. There are 42 sites (6 octahedral, 12 tetrahedral and 24 trigonal bipyramidal) available per unit cell for the two Ag^+ ions (in a unit cell) to occupy. The neutron diffraction studies[114,115] suggested that the Ag^+ ions resides mostly at the tetrahedral sites. This is supported by more recent studies.[116] The silver sublattice shows a very high degree of disorder and is 'liquid-like'.[1] This is because of the high density of energetically equivalent sites (tetrahedral sites) available in the lattice. Many authors[47,117–122] hold the view that ion-ion correlation is an important factor in bringing about the high sublattice disorder. It is suggested that the ion transport is via jump-diffusion process.[1]

One of the most interesting simulation studies on α-AgI is by Vashishta and Rahman.[94] They have developed a 'full' interionic potential for the study of AgI. Their molecular dynamics study employs an interionic potential given in 8.3. The study demonstrated that the structure and conductivity of α-AgI was well reproduced by the potential. Many interesting microscopic properties of the system are revealed in the study:

(1) Ag^+ occupies the tetrahedral sites;
(2) the long range motion of Ag^+ is through jumps between neighbouring tetrahedral sites and the majority (about 82%) of these jumps are found to be in the [110] direction;
(3) an Ag^+ resides at the tetrahedral sites for about 3 ps before it jumps to a neighbouring tetrahedral sites; and
(4) in the successive jumps Ag^+ has a bias towards backward jumps.

Later Parrinello *et al*[95] refined the parameters of the potential to reproduce the $\beta \leftrightarrow \alpha$ transition in AgI.[95] This is an excellent demonstration of how simulations can be made use of in the study of phase transitions in solids. Sekkal *et al*[123] have recently proposed a three-body potential for study of α-AgI under high pressure.

Another interesting study on ionic motion in α-AgI-type lattice is the computer aided calculation performed by Flygare and Huggins.[124] They examined the effect of the size (ionic radii) of the mobile ion on the activation energy barrier it encounters in the *bcc*-iodine sublattice of α-AgI. They observed that the activation barrier for ionic motion in the system varies anomalously with the ionic radius of the mobile ion.[124] This suggest that for a given framework of immobile lattice there is an optimum size ion – which is neither too big nor too small – that can diffuse faster.

Defect concentration and its influence on conductivity in β-AgI has been the subject of many interesting experimental[125,126] studies. Recent simulations studies by Zimmer *et al*[127] have been successful in providing better insight into the relation between the defect concentration and conductivity in this system.

9.1c *Ag_2 X-type (X = S, Se, Te):* The works of Vashishta *et al*[58,94] on AgI have been a great source of motivation to the researchers working in the field of computer simulation of superionic solids. Following their strategy silver ion conductors of the formula Ag_2X (where X = S,[96,128,129,] Se[130] and Te[131]) have also been investigated through computer simulations. As in α-AgI, the 'framework' ions in α-Ag_2S and α-Ag_2Se forms a thermally agitated *bcc* lattice while in α-Ag_2Te they (Te ions) are arranged in an *fcc* lattice like in the fluorite structure. Here α phase refers to the high-temperature-superionic phase. A few important contributions from simulation studies of these systems is briefly summarized below. The normal to superionic transition as well as many other structural and dynamical aspects of Ag_2S has been reproduced by simulations[96] in good agreement with experimental studies. The frequency dependent conductivity as well as the diffusion coefficient calculated in the simulation study[130] of Ag_2Se are in good agreement with experiments. The study[130] suggests that the Ag^+ ions largely occupy the tetrahedral sites of the bcc Se sublattice with only a small fraction occupying the octahedral sites. The simulation study[131] on α-Ag_2Te suggest that the conduction channel of Ag^+ ions is the one connecting a tetrahedral site to neighbouring octahedral site. The Haven ratio, H_R, expressed in (5) is a measure of the correlated motion of ions. In Ag_2Se and Ag_2S the value of H_R is found to be unusually low indicating high degree ion-ion correlations.[132] Monte Carlo simulations by Okazaki and Tachibana[133] suggest that the low value of H_R is probably due to 'caterpillar'-like motion (which is highly correlated) of Ag^+ ions in these systems. Similar correlated motion of Ag^+ is predicted in α-AgI as well.[134]

9.2 *Covalent framework solids*

The superionic solids with covalent framework consists of interconnected polyhedra, often tetrahedra or octahedra or both. They have high Debye temperature and the covalently bonded framework ions have high frequencies. These solids exhibit high melting temperatures as well. The β-aluminas ($M_2O.xAl_2O_3$, M = Li, Na, Ag etc.), NASICON ($Na_{1+x}Zr_2Si_xP_{3-x}O_{12}$), pyrochlore ($MSbO_3$, M = Na and K) etc. are good examples of superionic solids with covalent framework. Unlike the 'soft framework' superionic conductors most covalent framework solids do not show any sharp 'normal to superionic' transition. However, some of these (for example, $Na_3Zr_2Si_2PO_{12}$) do show a weak-second order-like transition where, at the transition temperature, the slope of the conductivity, when $\log(\sigma T)$ is plotted against $1/T$, changes. This suggests that the structural changes during the transition in these solids, if at all there is one, are of smaller magnitude compared to the soft framework solids. The superionic solids with covalent framework is of higher technological importance than those with soft framework as the former has much higher thermal and chemical stabilities. In practical applications of solid electrolytes it is important that the system does not undergo considerable structural changes near the operating temperature. This also favours the use of covalent framework superionic conductors in battery and similar applications.

9.2a *β and β''-alumina:* The β-aluminas ($M_2O.xAl_2O_3$, M = Li^+, Na^+, Ag^+, K^+, Rb^+ etc.) are known to be good ionic conductors after Yao and Kummer.[16] A large number of experimental[135–141] as well as theoretical[85–88,142–145] studies have been devoted to understand the structure, conductivity and nature of ionic motion in β-alumina. The β-alumina has a layered structure in which densely packed spinel blocks rich in Al_2O_3 are separated by loosely packed conduction planes where the mobile cations, M = Li, Na, etc. reside. The conduction planes also contain oxygens which bridge the spinel blocks. A wide range of cation substitution is possible in β-aluminas ($M_2O.xAl_2O_3$, M = Li^+, Na^+, K^+, Ag^+, Rb^+ etc.), of which, the Na-β-alumina has the highest conductivity and hence is the most widely studied of all. Though the ideal formula for the Na-β-alumina is $Na_2O.11Al_2O_3$, in practice, Na_2O content is larger than this by about ~25%.[137] Hence the formula is more appropriately, $Na_2O.(8–9)Al_2O_3$. Compositions still richer in Na_2O are referred to as β''-alumina whose formula is approximately $Na_2O.(5–7)Al_2O_3$. In β- and β''-alumina the spinel blocks are densely packed and provide no channels for alkali metal ions to move. Hence the alkali ions in these systems is confined to move only on the conduction planes which explains the two dimensional conductivity observed in them. β-aluminas are not known to exhibit any normal $\leftrightarrow$ superionic transition.

One of the interesting phenomenon observed in β-aluminas, $M_2O.xAl_2O_3$ where M = Li^+, Na^+, Ag^+, K^+ and Rb^+, is the activation energy of conduction varies anomalously with the size (ionic radius) of the *M* ion-substituted.[1] It may be noticed that the ionic radii

of the M ions increases in the order $Li^+ < Na^+ < Ag^+ < K^+ < Rb^+$. Still the Na^+-substituted system exhibits a higher conductivity than that of the other M ion substituted systems. This suggests that probably there is an optimum size of the mobile ion (M ion) whose diffusion is best favoured by the framework. The possibility of similar observation suggested by Flygare and Huggins[124] was discussed earlier in this previous section in the context of studies on AgI. The earliest computer aided calculation (the technique they have used is different from MD and MC) on *b*-aluminas is by Wang *et al.*[146] They have addressed this issue in good detail. They calculated potential energy variation along the conduction channel for each of these ions. It is clearly seen that the potential energy variation is less undulating for the Na^+ than the other ions. This rather flat potential energy surface seems to be associated with the maximum conductivity observed for the former.[146] Another important observation of Wang *et al*[146] is the correlated motion of the mobile ions in *b*-alumina.

A major breakthrough is the parameterization of the Born-Mayer-Huggins potential by Walker and Catlow for *b* and *b*²-alumina.[85] The potential parameters suggested by Walker and Catlow[85] was then made use of in many computer simulation studies that followed. These studies have provided much insights into the ionic motion and conduction mechanism in *b*-aluminas (*b* or *b*²-alumina). Thomas[143] has discussed how molecular dynamic simulation can be conveniently used as a complementary technique to conventional X-ray diffraction experiments to deduce microscopic mechanism in *b*-alumina.

One of the much discussed aspect in Na-*b* and *b*²-alumina are the Na^+ occupancies at the various alkali ion sites. There are three alkali ion sites in the conduction channel of these solids, which are, Beevers-Ross (BR), anit-Beevers-Ross (aBR) and mid-oxygen (mO) sites.[135] The exact compositions (Na_2O content) can be one of the factors that influence the occupancy of Na^+ at the various alkali ion sites. And it appears to be difficult to determine the exact Na_2O content in the Na-*b*-alumina. In the case of stoichiometric Na-*b*-alumina, spectroscopic evidence[147,148] suggests occupancy of the BR sites which are supported by calculation of crystal energetics by Catlow and Walker.[149] Leeuw and Perram[86] has employed molecular dynamics calculations on both stoichiometric and non-stoichiometric (where 25% excess Na_2O is present) *b*-alumina using the potential parameters given earlier.[85] For the stoichiometric system they observed Na^+ population at BR as well as mO sites and the Na^+ did not show any long range motion. This supports previous experimental result thereby suggesting that the conductivity of stoichiometric *b*-alumina is far less compared to the non-stoichiometric compound.[147] Another of their interesting observation is that an extra Na^+ added into the system (i.e., introducing non-stoichiometry) occupies the aBR sites and results in a sudden increase in Na^+ diffusivity. Extensive molecular dynamics calculation has been carried out by Walker and Catlow[85] on *b* as well as *b*²-alumina. Various bulk properties, like elastic constants, dielectric constants, lattice energies etc., of the system deduced from simulations are found to be in good agreement with experimental results. Many microscopic quantities of interest, like the defect energies associated with various Na^+ and O^- sites have been calculated for *b* as well as *b*²-alumina. The activation energy for conduction calculated in their study appears to be higher than that reported in experiments. The Na^+ conduction mechanism is proposed to be similar to vacancy mechanism in both *b* and *b*²-alumina.

Another interesting simulation study on Mg^{+2} stabilized *b*²-alumina ($Na_{2-x}Mg_{1-x}Al_{10+x}O_{17}$) is by Smith and Gillan.[87] They have studied the system at two non-stoichiometric compositions, $x = 1/3$ and $x = 1/4$, using a much larger system size than previous studies. Few of the particularly noteworthy results of their study is,

(1) the non-Arrhenius behaviour of the conductivity variation is well reproduced in their simulation;
(2) a spontaneous formation of the 'vacancy superlattice' (which refers to ordering of the Na^+ vacancy) is observed at low temperatures which is in good agreement with X-ray diffraction studies by Boilot *et al*;[150]
(3) the symmetry of the superlattice is found to depend crucially on the vacancy concentration;
(4) it is suggested that there is a dynamic making and breaking of the vacancy superlattice.

The study finds that larger system size needs to be employed in simulations to obtain reliable results.

Hafskjold and Li[88] also have carried out extensive molecular dynamics simulations of Mg stabilized *b*²-alumina of the formula ($Na_{1+x}Mg_xAl_{11-x}O_{17}$) with $x = 2/3$ and 3/4. The interesting observations of their study is that the distribution of Mg^{+2} in the spinel block has strong influence on,

(1) the stability of the Na^+ vacancy superlattice, and
(2) the diffusion coefficient of Na^+ (changes in diffusion coefficient can be up to an order of magnitude higher for optimum distribution of Mg^{+2}) also explains why the conductivity strongly depends on the thermal history of the sample.

It is also interesting to note that they observe high ion–ion correlation in the system. They propose this to be the main reason for the low activation energy for conduction in b''-alumina. The Haven ratio calculated also support this observation. Mixed alkali effect in b and b''-alumina has also been the subject of interesting simulation studies.[144]

10. NASICONs

After the discovery of b-alumina by Yao and Kummer,[16] a two-dimensional superionic conductor (SIC) with a fairly rigid Al_2O_3 framework and high density of well connected interstitial sites, it was postulated that compounds with similar frameworks but with three-dimensionally connected interstitial sites would be ideal candidates as solid electrolytes for battery and similar applications. The discovery of NASICON (for Na SuperIonic CONductor) by Hong[24] and Goodenough *et al*[25] is undoubtedly a major breakthrough in the direction of tailored making of fast ion conductors with a covalent framework structure. In his pioneering work Hong demonstrated that it is possible to synthesize a series of materials of the general formula $Na_{1+x}Zr_2Si_xP_{3-x}O_{12}$ with $0 \leq x \leq 3$ and that the material $Na_3Zr_2Si_2PO_{12}$ (the composition with $x = 2$) is an excellent ionic conductor. The conductivity of $Na_3Zr_2Si_2PO_{12}$ above 443 K was found to be comparable to that of Na-b-alumina ($Na_2O.xAl_2O_3$), with many a advantage in practical applications as fast ion conductor.[24] Henceforth materials with similar topology and structure as that of $Na_3Zr_2Si_2PO_{12}$ are referred to as NaSICons (for Na-SuperIonic Conductors), or simply NASICONs, irrespective of whether Na^+ or other ions are present and whether they classify as superionic conductors or not. Apart from being potential candidates as solid electrolytes, NASICON-type materials find enormous applications in conversion systems, supercapacitors,[151,152] sensors[153] displays,[154] nuclear waste disposals,[155,156] as low expansion ceramics,[156–163] and thermal-shock-resistant materials.[164] Recently the porous glasses of NASICONs have been found to show promising catalytic activities as well.[165,166]

10.1 *Synthesis*

NASICONs can be synthesized by conventional ceramic methods including solid state reaction method (or powder mixing), solution-sol-gel method, or hydrothermal method. Ion exchanges are also employed.[167] The sol–gel method is found to be better in most cases because the mixing of the components is achieved at molecular level. The hydrothermal method provides a low temperature route for synthesis of ultra-fine powders of $NaZr_2(PO_4)_3$.[156]

10.1a *Solid state reaction route:* Stoichiometric amounts of the dry powders of Na_2CO_3, ZrO_2 and $NH_4H_2PO_4$ are mixed. The mixture is then hand ground, air dried and preheated at around 170°C for 4 h. It is then calcined to remove the volatiles such as CO_2, NH_3 and H_2O at 600°C for another 4 hours and at 900°C for 16 h. Intermediate grinding and mixing improves the homogenization of the powder. The calcined powder is then sintered at 1200–1500°C to get good crystallinity for the product.[24,156]

10.1b *Sol–gel route:* Stoichiometric amounts of alkali nitrate and $ZrOCl_2$ are mixed at constant stirring conditions at room temperature. The H_3PO_4 is added slowly. The gel is dried at 90°C for 24 h and then calcined at 700°C for 16 h. The calcined powder is then sintered at 1200–1500°C to get good crystallinity for the product.[156,168]

10.1c *Hydrothermal method:* Stoichiometric amounts of alkali nitrate or chloride is dissolved in 0·5M $ZrOCl_2$ solution and the H_3PO_4 is added drop by drop while stirring. The gel is dried at 70°C and heat treated at 170–230°C for 24 h. The solution phase is then separated off the product by centrifugation. The solid phase obtained is washed and dried to get a fine powder of $NaZr_2(PO_4)_3$.[156,169,170]

10.2 *Structure of $NaZr_2(PO_4)_3$*

The $NaZr_2(PO_4)_3$ is prototypical of NASICONs and it stabilizes in the rhombohedral $R\bar{3}c$ space group. The first report of the crystal structure of $NaZr_2(PO_4)_3$ was by Hagman and Kierkegaard[171] in 1968. The crystal structure of $NaZr_2(PO_4)_3$, the prototype of NASICONs, consists of a three-dimensional framework of corner-shared ZrO_6-octahedra and PO_4-tetrahedra. This $[Zr_2(PO_4)_3]^-$-framework is highly stable due to its covalent nature and shows high

melting points (> 1650°C). The basic unit of the framework consists of two ZrO_6-octahedra and three PO_4-tetrahedra corresponding to $[Zr_2(PO_4)_3]^-$. Each ZrO_6-octahedron is connected to three PO_4-tetrahedra, each of which is linked to four ZrO_6-octahedra. These units in turn are connected to form 'ribbons' along the *c*-axis and the ribbons are joined together along the *a*- and *b*-axis by PO_4-tetrahedra. Figure 1 shows a view of the $NaZr_2(PO_4)_3$-structure parallel to the *c*-axis.

The corner sharing, rather than edge sharing, of the ZrO_6 and PO_4 polyhedra gives rise to a fairly open framework structure with structural holes.[156] The presence of the structural holes render the polyhedra some freedom for rotational motion.[156] Many interesting properties of NASICONs, like the low and anisotropic thermal expansion, high shock resistive nature, flexibility to incorporate ions of varying sizes etc., are often attributed to the presence of structural holes.

10.2a *Na^+ sites in $NaZr_2(PO_4)_3$*: There are mainly two types of sites present in the structure of $NaZr_2(PO_4)_3$, which are often referred to as Na(1) (the 6b positions of $R\bar{3}c$) and Na(2) (18e positions of $R\bar{3}c$). The Na(1) and Na(2) sites are shown in figure 1 as filled circle (•) and open circle (○), respectively. The Na(1) sites are located between two ZrO_6-octahedra along the *c*-axis. The Na(2) sites are located between the ribbons of the ZrO_6-octahedra. The Na(1) site is in regular six coordination with oxygens forming $Na(1)O_6$ octahedra while the Na(2) site is irregularly eight coordinated with oxygens (these oxygens are shown connected to their respective sites by a stick in figure 2). Apart from these two sites there is yet another site located midway between an Na(1) and its neighbouring Na(2) site. This site, referred to as mid-Na site (36*f* positions of $R\bar{3}c$) is five-coordinated with oxygens and has the shortest average Na-O distance. The mid-Na site (see figure 2) is identified only in certain NASICONs, like $LiZr_2(PO_4)_3$ and $Na_3Zr_2Si_2PO_{12}$ etc.[173,174] There are one Na(1), three Na(2) and six mid-Na sites per unit formula ($NaZr_2(PO_4)_3$) and one unit cell consists of six formula units. These sites are interconnected in three dimensions giving rise to a three dimensional network of the conduction channel. An Na(1) is six-coordinated with Na(2) sites which are two coordinated with Na(1) sites. The mid-Na site is located mid-way in the conduction channel connecting an Na(1) and an Na(2). In $NaZr_2(PO_4)_3$ the Na^+ occupies only the Na(1) sites at room temperature.

10.2b *Geometrical bottlenecks for the motion of Na^+:* The identification of the conduction channel in the structure and the bottlenecks (to ionic motion) in it, is important for an understanding of the nature of ionic motion in solid electrolytes. Two distinct conduction channels (pathways or hop path of ions) are proposed to exist in the rhombohedral-$R\bar{3}c$ struc-

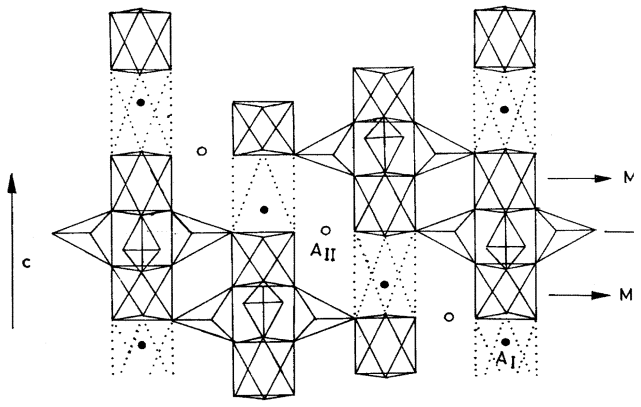

Figure 1. A view of the $NaZr_2(PO_4)_3$-structure parallel to the *c* axis. The corner-shared ZrO_6-octahedra and PO_4-octahedra as well as the Na(1), shown as filled circle (•), and Na(2), shown as open circle (○), can be seen (taken from ref. 172).

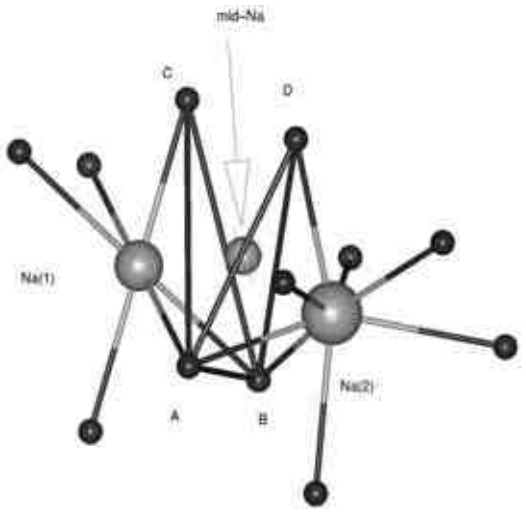

Figure 2. A magnified view of the oxygen environment around the Na(1)–Na(2) conduction channel is shown. The Na(1), Na(2) and mid-Na sites as well as the oxygen neighbours at Na(1) and Na(2) (shown connected to the respective sites by sticks) can be seen. The oxygen atoms forming the bottlenecks are marked A, B, C and D with triangles A-B-C and A-B-D representing the first and the second bottlenecks, respectively.

ture of NASICONs.[175] The first of these is connecting an Na(1) to its neighbouring Na(2) site while the second connects two neighbouring Na(2) sites. It appears that an Na(1)–Na(1) path does not exist. Tran Qui *et al*[175] analysing $Na_4Zr_2Si_3O_{12}$ find that the bottleneck in the conduction channel connecting two neighbouring Na(2) sites is formed by trapezoidal arrangement of oxygen atoms and is wider than the triangular bottleneck of oxygens in the Na(1)–Na(2) conduction channel. Kohler and Schulz[176] have carefully investigated the bottlenecks in the Na(1)–Na(2) conduction channel of rhombohedral NASICON structure. They showed that there are two bottlenecks in this conduction channel which are situated approximately at 1·2 Å and 2·21 Å from Na(1) site. Both the bottlenecks are formed by triangular arrangement of oxygen. The first bottleneck (the one closer to Na(1)) is formed by oxygen atoms of the $Na(1)O_6$ octahedra (marked A-B-C in figure 2). The second bottleneck (marked A-B-D in figure 2) lies closer to Na(2) and shares an edge (AB) with the first one. The dimensions as well as the exact position of the bottlenecks vary with changes in the framework due to change in composition, temperature, etc.

10.3 *Properties of NASICONs*

The NASICONs exhibit many useful as well as interesting properties which are often attributed to their unique structural features. Some of the properties of NASICONs which make them a technologically important material will be briefly discussed below.[177]

10.3a *Chemical substitution:* The flexibility of the $[Zr_2(PO_4)_3]^-$-framework of $NaZr_2(PO_4)_3$ allows substitution of various ions at each of the Na, Zr and P sites. Thus a variety of crystalline materials have been synthesized and characterized. Most of these are iso-structural to the $NaZr_2(PO_4)_3$.[24,35,164,178–196] Apart from these, amorphous materials of NASICON compounds have also been synthesized and characterized by different groups.[197–208] Table 1 gives a list of ions which can be substituted at the various Na, Zr and P sites of $NaZr_2(PO_4)_3$.

The most important aspect of these solids is that the oxygen ions in the framework cannot be removed or transported across. Substitution of ions of higher oxidation states at the Zr and P sites increases the strength of the framework. This also widens the choice of ions that can be substituted at the Na sites.[209]

10.3b *High thermal and chemical stability:* Owing to their strong, covalently bonded 3-dimensional framework NASICONs exhibit relatively high melting points (>1650°C).[156] On the reactivity of these solids, due to the high covalent nature of the framework the reactions involving the skeleton take place at much higher temperatures than those involving the counter-ions.[209] They also show high chemical stability and good mechanical strength.[156]

10.3c *High ionic conductivity:* NASICONs have a high density of interstitial sites with three-dimensional connectivity across them. Hence, when substituted with smaller alkali ions like, Li^+ and Na^+, they show excellent ionic conductivity. This along with their high thermal stability and low thermal expansivity make them excellent candidates as solid electrolytes in battery applications. $Na_3Zr_2Si_2PO_{12}$ is an excellent superionic conductor (SIC) and above 420 K its conductivity is comparable to that of the Na *b*-alumina. The NASICONs have the advantage of near isotropic conductivity over the *b*-alumina. $LiZr_2(PO_4)_3$ is a good superionic conductor (SIC), above 620 K, which finds applications in high-energy-density storage devices.

10.3d *Low thermal expansion:* The low thermal expansivity of NASICONs has been known for some time.[210] NASICONs in general exhibit low and anisotropic thermal expansions.[209–211] For example, $NaZr_2(PO_4)_3$ shows an average thermal expansivity of $-5{\cdot}4 \times 10^{-6}°C^{-1}$ along the *a*-axis and $22{\cdot}4 \times 10^{-6}°C^{-1}$ along the *c*-axis over the temperature range of 300–1000 K. The low thermal expansivity of NASICONs are attributed to (i) the strongly bonded framework structure and (ii) the presence of structural holes in

Table 1. A non-exhaustive list of ions that can be substituted at the Na, Zr and P sites of $NaZr_2(PO_4)_3$.

Site	Ions that can be substituted
Na	H^+, Li^+, K^+, Rb^+, Cs^+, NH_4^+, Cu^+, Ag^+, Tl^+, H_3O^+, Mg^{+2}, Ca^{+2}, Sr^{+2}, Ba^{+2}, Mn^{+2}, Co^{+2}, Zn^{+2}, Pb^{+2}, Fe^{+3}, La^{+3}…
Zr	Na^+, Ti^{+4}, Ge^{+4}, Sn^{+4}, Th^{+4}, U^{+4}, Nb^{+4}, V^{+3}, Cr^{+3}, Fe^{+3}, Co^{+3}, Ga^{+3}, In^{+3}, Mg^{+2}, Mn^{+2}, Cu^{+2}, Zn^{+2}, Ni^{+2}…
P	Si^{+4}, As^{+5}, S^{+6}…

the structure.[156] It is suggested that the structural holes enable the PO_4-tetrahedra and ZrO_6-octahedra to rotate in a coupled fashion enabling the material to take up the thermal strain without appreciable lattice expansion.[162,163,209] Near zero-thermal expansion materials of NASICON family have been synthesized through incorporation of suitable ions like Ca, Sr or Ba in the alkali ion sites[155–157,212,213] or by replacing few of the tetravalent ions (Zr ions) by Na ions.[160] A solid solution between two materials with opposite thermal expansion behaviour also has been used to develop low thermal expansion ceramics.[156]

10.4 *Recent insights from computer simulation investigations*

As already pointed out, molecular simulations can provide valuable insights into the microscopic properties as well as provide its interrelationship with the changes in the macroscopic properties. Recently, we have studied some of the NASICON structures to understand their properties especially at the molecular level. Obtaining an insight at the microscopic level has been difficult and there exist many unresolved questions, for which these molecular simulations can be useful.

One of the intriguing observations is the conductivity maximum as a function of composition seen in $Na_{1+x}Zr_2Si_xP_{3-x}O_{12}$ with $0 \le x \le 3$. In this class of systems, it is seen that the conductivity is a maximum around $x = 2{\cdot}0$. In order to understand the processes controlling conductivity at the atomic level, it is desirable to carry out detailed molecular dynamics simulations of these systems. For this, however, accurate intermolecular interaction potential is required. Such a potential was recently proposed.[214] The form of the potential is:

$$U(r_{ij}) = \frac{q_i q_j}{r_{ij}} + \frac{A_{ij}(s_i + s_j)^{n_{ij}}}{r_{ij}^{n_{ij}}} - \frac{C_{ij}}{r_{ij}^6}.$$

This potential does not assume a rigid framework of NASICON but provides a full potential wherein interactions between ions within the framework as well as outside the framework are taken into account. This potential could reproduce accurately both the variation of lattice parameters as well as conductivity with composition. With the availability of this potential, it is possible to study the properties of the NASICON through simulations. Further, it is also possible to investigate changes in framework structure with nature of the cation, composition, temperature, etc.

A detailed molecular dynamics study of the composition dependence of the structure, conductivity and ion motion in $Na_{1+x}Zr_2Si_xP_{3-x}O_{12}$ employing the above potential has been recently reported.[215] Constant-pressure, constant-temperature variable-shape simulation cell Monte Carlo and microcanonical ensemble molecular dynamics simulation of superionic conducting rhombohedral phase of NASICON, $Na_{1+x}Zr_2Si_xP_{3-x}O_{12}$ with $0 \le x \le 3$, at a temperature of 600 K is reported. Changes in structure, conductivity, hop path, site occupancies, bond lengths of framework atoms with composition are discussed. Average Na(1)–O distance shows a peak at $x = 2$, while Na(2)–O distance shows a monotonic increase. Sum of the sodium occupancies at Na(1) and mid-Na sites add up to a constant value of unity which supports the conclusion of Boilot *et al*[216] based on X-ray diffraction. Occupancy of the Na(1) site attains a minimum at $x = 2$. The predominant conduction channel (which carries more than 90% of the sodium ions) is found to be the one connecting Na(1)-mid-Na-Na(2). Density contours for sodium, depicting this conduction channel, are reported. Free energy profile along the conduction channel suggests that entropy contribution cannot be neglected. The mid-Na site is not associated with a free energy minimum.

An interionic potential to investigate Li ion motion in the rigid framework of PO_4 tetrahedra and ZrO_6 octahedra of $LiZr_2(PO_4)_3$ – a Nasicon-type superionic conductor – has been developed by fitting to the low-temperature X-ray structure and conductivity data at 700 K.[217] A molecular dynamics simulation employing this potential function has been carried out. A detailed analysis of the molecular dynamics trajectories suggests that the proposed interionic potential can predict properties of the $LiZr_2(PO_4)_3$ in good agreement with known X-ray, NMR, calorimetric, conductivity, and other data. The transition from normal to superionic conductor takes place between 550 and 600 K and is accompanied by a peak in the constant volume specific heat, suggestive of a higher order transition as well as migration of Li ions from crystallographic 6b (site 1) to 18e (site 2) position. The activation energy and path of migration of Li ions from site 1 to 2 are in good agreement with experiment. Density contours surrounding sites 1 and 2, which reveal the exact geometry of the void

space around these sites, are in excellent qualitative agreement with thermal ellipsoid parameters obtained from X-ray diffraction. The frequency of vibration of Li ion in the two sites are found to depend strongly on the geometry of the void space at these sites dictated by the potential energy surface.

In order to find out the underlying cause for the conductivity maximum, a model study was carried out in which ion radius was varied over a range without constraining the radius of the ion to the real ions.[218] A molecular dynamics study of ion mobility as a function of the size of the mobile ion within Nasicon-type structures was carried out. The self diffusivity exhibits an anomalous peak suggesting that the levitation effect exists even in ionic systems dominated by Coulomb interaction. This has important consequences in the diffusion of ions in chemical and biological systems. It is seen that high mobility of the ion is associated with the liquid-like radial distribution functions between the ion and the oxygen of the framework. The force on the ion due to the framework within which it is moving is found to be a minimum.

10.5 *Technological applications of NASICONs*

NASICONs find their applications in diverse fields. A few are listed below.

- solid electrolytes
- low thermal expansion ceramics
- substrate materials for electronic packaging
- oxidation protection coatings of non-oxide materials
- nuclear waste disposal
- catalysis.

11. Conclusions

We have provided a summary of experimental, computational and sometimes theoretical studies on solid-state ionic conductors. It appears that the solid state ionic conductors are superior to liquid electrolytes in several ways. The reasons for this is not difficult to appreciate. The disorder in these crystalline solids is significantly less than that seen in liquids.

There still remain certain aspects that need to be investigated. These are the microscopic nature of the ionic motion, the normal to superionic phase transitions, the dependence of diffusivity on the size of the diffusing species, the changes in the zirconium silico phosphate-framework upon the variation of size and the content of alkali ion and the role of framework expansions as well as vibrations on conductivity.

Acknowledgement

The authors thank the Department of Science and Technology, New Delhi for financial support.

References

1. Chandra S 1981 *Superionic solids principles and application* (Amsterdam: North-Holland)
2. Bruce P (eds) 1995 *Solid state electrochemistry* (New York: Cambridge University Press)
3. Faraday M 1838 *Philos. Trans. R. Soc. London* (London: Richard and J Taylor)
4. Warburg E 1994 *Ann. Phys. Chem. N. F.* **21** 662
5. Warburg E and Tegetmeier F 1888 *Ann. Phys. Chem. NF* **32** 455
6. Nernst W 1900 *Z. Electrochem.* **6** 41
7. Tubandt C and Lorenz E 1914 *Z. Phys. Chem.* **87** 513
8. Katayama M 1908 *Z. Phys. Chem*. **61** 566
9. Bauer E and Preis H 1937 *Z. Electrochem.* **44** 727
10. Kiukkola K and Wagner C 1957 *J. Electrochem. Soc.* **104** 379
11. Reuter B and Hardel K 1961 *Naturwissenschaften* **48** 161
12. Owens B B and Argue G R 1967 *Science* **157** 308
13. Bradley J N and Green P D 1967 *Trans. Farad. Soc.* **63** 424
14. Takahashi T and Yamamoto O 1966 *Electrochem. Acta* **11** 779
15. Argue G R and Owens B B 1968 *Abstracts, 133rd National Meeting of the Electrochemical Society*, Boston, MA, No. 281
16. Yao Y F and Kummer J T 1967 *J. Inorg. Nucl. Chem.* **29** 2453
17. Kummer J T and Weber N 1966 *US Patent* **3** 458 356
18. Kuwabara K and Takahashi T 1976 *J. Solid State Chem.* **19** 147
19. Boilot J P, Thery J and Collongues R 1973 *Mater. Res. Bull*. **8** 1143
20. Takahashi T, Kuwabara K and Kase Y 1975 *Denki Kagaku* **43** 273
21. Takahashi T, Kuwabara K and Kase Y 1975 *Nippon Kagaku* **8** 1305
22. Delmas C, Fouassier C, Reau J M and Hagenmuller P 1976 *Mater. Res. Bull*. **11** 1081
23. Trichet L and Rouxel J 1977 *Mater. Res. Bull.* **12** 345
24. Hong H Y-P 1976 *Mater. Res. Bull*. **11** 173
25. Goodenough J B, Hong H Y-P and Kafalas J A 1976 *Mater. Res. Bull.* **11** 203
26. Benrath A and Drekopt K 1921 *Z. Phys. Chem.* **99** 57

27. Førland T and Krogh-Moe J 1957 *Acta. Chem. Scand.* **11** 565
28. Kvist A and Lunden A 1965 *Z. Naturforsch.* **A20** 235
29. Heed B 1975 *Dissertation*, Gothenburg
30. West A R 1973 *J. Appl. Electrochem.* **3** 327
31. Garcia A, Torres-Trevino G and West A R 1990 *Solid State Ionics* **40/41** 13
32. Huggins R A 1977 *Electrochim. Acta* **22** 773
33. Boukamp B A and Huggins R A 1976 *Phys. Lett.* **A58** 231
34. Roth W L and Farrington G C 1977 *Science* **196** 1332
35. Taylor B E, English A D and Berzins T 1977 *Mater. Res. Bull.* **12** 171
36. Tell B, Wagner S and Kasper H M 1977 *J. Electrochem. Soc.* **124** 536
37. Réau J M, Magniez G, Rabardel L, Chaminade J P and Pouchard M 1976 *Mater. Res. Bull.* **11** 867
38. Angell C A 1989 *High conductivity solid ionic conductors* (ed.) Takahashi (Singapore: World Scientific)
39. Souquet J L and Kone A 1986 *Materials for solid state batteries* (eds) B V R Chowdari and S Radhakrishna (Singapore: World Scientific)
40. Souquet J L 1995 *Solid state electrochemistry* (ed.) P G Bruce (New York: Cambridge Univ. Press)
41. Tonge J S and Shriver D F 1989 *Polymer for electronic applications* (ed.) J H Lai (Boca Raton FL: CRC Press)
42. Cowie J M G and Cree S H 1989 *Annu. Rev. Phys. Chem.* **40** 85
43. Linford R G (eds) 1990 *Electrochemical Science and Technology of Polymers* **2**
44. Bruce P G and Vincent C A 1993 *J. Chem. Soc., Faraday Trans.* **89** 3187
45. Rice M J and Roth W L 1972 *J. Solid State Chem.* **4** 294
46. Beniere F 1972 *Physics of electrolytes* (ed.) J Hladik (New York: Academic Press)
47. Lederman F L, Salamon M B and Peisl H 1976 *Solid State Commun.* **19** 147
48. Funke K and Hackenberg R 1971 *Ber. Bunsenges. Phys. Chem.* **75** 436
49. Knotek M L and Seager C H 1977 *Solid State Commun.* **21** 625
50. Knotek M L 1976 *J. Electrochem. Soc.* **123** 756
51. von Neumann J and Ulam S 1945 *Bull. Am. Math. Soc.* **51** 660
52. Metropolis N, Rosenbluth A W, Rosenbluth M N, Teller A H and Teller E 1953 *J. Chem. Phys.* **21** 1087
53. Reif F 1992 *Fundamentals of statistical and thermal physics* (New York: McGraw-Hill)
54. Allen M P and Tildesley T J 1987 *Computer simulation of liquids* (Oxford: Clarendon)
55. Frenkel D and Smit B 1996 *Understanding molecular simulations: from algorithms to applications* (San Diego: Academic Press)
56. McDonald I R 1980 *Mol. Phys.* **23** 41
57. Andersen H C 1980 *J. Chem. Phys.* **72** 2384
58. Parrinello M and Rahman A 1980 *Phys. Rev. Lett.* **45** 1196
59. Parrinello M and Rahman A 1981 *J. Appl. Phys.* **52** 7182
60. Norman G E and Filinov V S 1969 *High Temp.* (*USSR*) **7** 216
61. Adams D J 1975 *Mol. Phys.* **29** 307
62. Alder B J and Wainwright T E 1957 *J. Chem. Phys.* **27** 1208
63. Alder B J and Wainwright T E 1959 *J. Chem. Phys.* **31** 459
64. Rahman A 1964 *Phys. Rev.* **A136** 405
65. Goldstein H 1993 *Classical mechanics* (New Delhi: Narosa)
66. Nosé S 1984 *Mol. Phys.* **52** 255
67. Nosé S 1984 *J. Chem. Phys.* **81** 511
68. Hoover W G 1985 *Phys. Rev.* **A 31** 1695
69. Hoover W G 1986 *Phys. Rev.* **A34** 2499
70. Hansen J P and McDonald I R 1986 *Theory of simple liquids* 2nd edn (New York: Academic Press)
71. Brown I D 1992 *Z. Kristallogr.* **199** 255
72. Kohn W and Sham L J 1965 *Phys. Rev.* **140** A1133
73. Car R and Parrinello M 1985 *Phys. Rev. Lett.* **55** 2471
74. Feynman R P and Hibbs A R 1965 *Quantum mechanics and path integrals* (New York: McGraw Hill)
75. Barker J A 1979 *J. Chem. Phys.* **70** 2914
76. Thirumalai D and Berne B J 1983 *J. Chem. Phys.* **79** 5029
77. Tosi M P and Fumi F G 1964 *J. Phys. Chem. Solids* **25** 45
78. Fumi F G and Tosi M P 1964 *J. Phys. Chem. Solids* **25** 31
79. Adams D J and McDonald I R 1974 *J. Phys.* **C7** 2761
80. Lewis J W E, Singer K and Woodcock L V 1975 *J. Chem. Soc., Faraday Trans. II* **71** 301
81. Woodcock L V 1971 *Chem. Phys. Lett.* **10** 257
82. Sangster M J L and Dixon M 1976 *Adv. Phys.* **25** 247
83. Hansen J P and McDonald I R 1974 *J. Phys.* **C7** L384
84. Gillan M J and Dixon M 1980 *J. Phys.* **C13** 1901
85. Walker J R and Catlow C R A 1982 *J. Phys.* **C15** 6151
86. De Leeuw S W and Perram J W 1979 *Fast ion transport in solids electrodes and electrolytes* (eds) Vashishta, Mundy and Shenoy (North Holland New York: Elsevier)
87. Smith W and Gillan M J 1992 *J. Phys.: Condens. Matter.* **D4** 3215
88. Hafskjold B and Li X 1995 *J. Phys.: Condens. Matter.* **D7** 2949
89. Wolf M L, Walker J R and Catlow C R A 1984 *J. Phys.* **C17** 6623
90. Wolf M L and Catlow C R A 1984 *J. Phys.* **C17** 6635
91. Wilde P J and Catlow C R A 1998 1998 *Solid State Ionics* **112** 185
92. Ammundsen B, Burns G R, Islam M S, Kanoh H and Roziére J 1999 *J. Phys. Chem.* **B103** 5175

93. Islam M S 2000 *J. Mater. Chem.* **10** 1027
94. Vashishta P and Rahman A 1978 *Phys. Rev. Lett.* **40** 1337
95. Parrinello M, Rahman A and Vashishta P 1983 *Phys. Rev. Lett.* **50** 1073
96. Ray J R and Vashishta P 1989 *J. Chem. Phys.* **90** 6580
97. Gillan M J 1985 *Physica* **B131** 157
98. Catlow C R A 1990 *J. Chem. Soc., Faraday Trans.* **86** 1167
99. Catlow C R A 1992 *Solid State Ionics* **53–56** 955
100. Ratner M A and Nitzan A 1988 *Solid State Ionics* **28–30** 3
101. Schoonman J, Ebert L B, Hsieh C H and Huggins R A 1973 *J. Appl. Phys.* **46** 2873
102. Bonne R W and Schoonman J 1977 *J. Electrochem. Soc.* **124** 28
103. Kennedy J H and Miles R C 1976 *J. Electrochem. Soc.* **123** 47
104. Derrington C E and O'Keeffe M 1973 *Nature* (*London*) **246** 44
105. Rahman A 1976 *J. Chem. Phys.* **65** 4845
106. Kim Y S and Gordon R G 1974 *J. Chem. Phys.* **60** 4332
107. Jacucci G and Rahman A 1978 *J. Chem. Phys.* **69** 4117
108. Dixon M and Gillan M J 1980 *J. Phys.* **C13** 1919
109. Dixon M and Gillan M J 1980 *J. de Physique* **41** C6
110. Montani R A 1994 *J. Chem. Phys.* **100** 8381
111. Walker A B, Dixon M and Gillan M J 1982 *J. Phys.* **C15** 4061
112. Castiglione M J, Wilson M, Madden P A and Grey C P 2001 *J. Phys.* **D13** 51
113. Funke K 1976 *Prog. Solid State Chem.* **11** 345
114. Buhrer W and Halg M 1974 *Helv. Phys. Acta* **47** 27
115. Wright A F and Fender B E F 1977 *J. Phys.* **C10** 2261
116. Yoshiasa A, Maeda H, Ishii T and Koto K 1990 *Solid State Ionics* **40/41** 341
117. Huberman B A 1974 *Phys. Rev. Lett.* **32** 1000
118. Rice M J, Strassler S and Toombs G A 1974 *Phys. Rev. Lett.* **32** 596
119. Pardee W J and Mahan G D 1975 *J. Solid State Chem.* **15** 310
120. Vergas R, Salamon M B and Flynn C P 1976 *Phys. Rev. Lett.* **37** 1550
121. Salamon M B 1977 *Phys. Rev.* **B15** 2236
122. Welch D O and Dienes G J 1977 *J. Phys. Chem. Solids* **38** 311
123. Sekkal W, Laref A, Zaoui A, Aourag H and Certier M 1999 *Solid State Commun.* **112** 49
124. Flygare W H and Huggins R A 1973 *J. Phys. Chem. Solids* **34** 1199
125. Hainovsky N and Maier J 1995 *Phys. Rev.* **B51** 15789
126. Lee J-S, Adams S and Maier J 2000 *J. Phys. Chem. Solids* **61** 1607
127. Zimmer F, Ballone P, Maier J and Parrinello M 2000 *J. Chem. Phys.* **112** 6416
128. Ihara S and Suzuki K 1984 *J. Phys. Soc. Japan* **53** 3081
129. Vashishta P, Ebbsjö I, Dejus R and Sköld K 1985 *J. Phys.* **C18** L291
130. Rino J P, Hornos Y M M, Antonio G A, Ebbsjö I, Kalia R and Vashishta P 1988 *J. Chem. Phys.* **89** 7542
131. Tachibana F, Kobayashi M and Okazaki H 1988 *Solid State Ionics* **28–30** 41
132. Okazaki H 1976 *J. Phys. Soc. Japan* **23** 355
133. Okazaki H and Tachibana F 1988 *Solid State Ionics* **28–30** 495
134. Tachibana F and Okazaki H 1987 *Solid State Ionics* **23** 219
135. Peters C R, Bettman M, Moore J W and Glick M D 1971 *Acta. Crystallogr.* **B27** 1826
136. Radzilowski R H and Kummer J T 1971 *J. Electrochem. Soc.* **118** 714
137. Roth W L 1972 *J. Solid State Chem.* **4** 60
138. Kennedy J H 1977 In *Solid Electrolytes* (ed.) Geller (Berlin: Springer-Verlag)
139. Collongues R, Thery J and Boilot J P 1978 In *Solid electrolytes* (eds) P Hagenmuller and W van Gool (New York: Academic Press)
140. Davies P K, Gorson F, Feist T and Katzan C M 1986 *Solid State Ionics* **18/19** 1120
141. Takahashi T 1989 *High conductivity solid ionic conductors, recent trends and applications* (Singapore: World Scientific)
142. Wolf M L, Walker J R and Catlow C R A 1984 *Solid State Ionics* **13** 33
143. Thomas J O 1992 *Solid State Ionics* **53–56** 1311
144. Mayer M, Jaenisch V, Maass P and Bunde A 1996 *Phys. Rev. Lett.* **76** 2338
145. Wang Y and Cormack A N 1998 *Solid State Ionics* **111** 333
146. Wang J C, Gaffari M and Choi S 1975 *J. Chem. Phys.* **26** 772
147. Hayes W and Holden L 1980 *J. Phys.* **C13** L321
148. Colomban Ph and Lucazeau G 1980 *J. Chem. Phys.* **72** 1213
149. Catlow C R A and Walker J R 1980 *Nature* (*London*) **286** 473
150. Boilot J P, Collin G, Colomban Ph and Comes R 1980 *Phys. Rev.* **22** 5912
151. Sekido S and Ninimoya Y 1981 *Solid State Ionics* **3/4** 153
152. Pham-Thi M, Velasco G and Colomban Ph 1986 *J. Mater. Sci. Lett.* **5** 415
153. 1978 *Solid electrolytes* (New York: Academic Press)
154. Dautremont-Smith W C 1982 *Displays* **3** 3
155. Roy R, Vance E R and Alamo J 1982 *Mater. Res. Bull.* **17** 585
156. Agrawal D K 1996 *Trans. Indian Ceram. Soc.* **55** 1
157. Roy R, Agrawal D K, Alamo J and Roy R A 1984 *Mater. Res. Bull.* **19** 471
158. Roy R, Agrawal D K and McKinstry H A 1989 *Annu. Rev. Mat. Sci.* **19** 59
159. Agrawal D K 1994 *J. Mater. Educ.* **16** 139
160. Alamo J and Roy R 1984 *Commun. Am. Ceram. Soc.* **C67**
161. Lenain G E, McKinstry H A, Limaye S Y and Woodward A 1984 *Mater. Res. Bull.* **19** 1451

162. Alamo J and Roy R 1986 *J. Mater. Sci.* **21** 444
163. Lenain G E, McKinstry H A, Alamo J and Agrawal D K 1987 *J. Mater. Sci.* **22** 17
164. Oota T and Yamai I 1986 *J. Am. Ceram. Soc.* **69** 1
165. Yamamoto K, Kasuga T and Abe Y 1997 *J. Am. Ceram. Soc.* **80** 822
166. Yamamoto K and Abe Y 1998 *J. Am. Ceram. Soc.* **81** 2201
167. Nagai M, Nisino T and Kanazawa T 1986 *Solid State Ionics* **18/19** 964
168. Perthuis H and Colomban Ph 1986 *Ceram. Int.* **12** 39
169. Komarneni S 1988 *Int. J. High Tech. Ceram.* **4** 31
170. Yong Y and Wenqin P 1990 *J. Chem. Soc., Chem. Commun.* **10** 764
171. Hagman L and Kierkegaard P 1968 *Acta Chem. Scand.* **22** 1822
172. Bhuvaneswari G 1990 *Synthesis, structure and properties of NZP and related network phosphates*, PhD thesis, Indian Institute of Technology, Chennai
173. Catti M and Stramare S 2000 *Solid State Ionics* **136–137** 489
174. Boilot J P, Collin G and Colomban Ph 1988 *Mater. Res. Bull.* **73** 160
175. Tran Qui, D Capponi J J, Joubert J C and Shannon R D 1981 *J. Solid State Chem.* **39** 219
176. Kohler H and Schulz H 1985 *Mater. Res. Bull.* **20** 1461
177. Agrawal D K and Roy R 1997 *A White Paper* **1**
178. Clearfield A, Roberts B D and Subrahmanian M A 1984 *Mater. Res. Bull.* **19** 219
179. Sljukic M, Matkovic B, Prodic B and Scavnicar S 1967 *Croat. Chem. Acta Zagreb*. **39** 145
180. Masse R 1970 *Bull. Soc. Fr. Miner. Cristallogr.* **93** 500
181. Subramanian M A, Roberts B D and Clearfield A 1984 *Mater. Res. Bull.* **19** 1471
182. Cava G L, Vogel E M and Johnson Jr D W 1982 *J. Am. Ceram. Soc.* **65** C157
183. Matkovic B, Prodic B and Sljukic M 1968 *Bull. Soc. Chim. France* 1777
184. Perret R and Boudjada A 1976 *C. R. Acad. Sci. Paris* **C282** 245
185. Delmas C, Olazcuaga R, Cherkaoui F, Brochu R and Le Flem G 1978 *C. R. Acad. Sci. Paris* **C287** 169
186. Alamo J and Roy R 1984 *J. Solid State Chem.* **51** 270
187. Senbhagaraman S, Guru Row T N and Umarji A M 1989 *Solid State Commun.* **71** 609
188. Sugantha M, Varadaraju U V and Subba Rao G V 1994 *J. Solid State Chem.* **111** 33
189. Kryukova A I, Korshunov I A, Moskvichev E P, Mitrofanova V A, Voroíbeva N V, Kazantsev G N and Skiba O V 1976 *Russ. J. Inorg. Chem.* **21** 1048
190. Chernorukov N G, Korshunov I A and Prokofeva T V 1978 *Sov. Phys. Crystallogr.* **24** 475
191. Byrappa K, Gopalakrishna G S, Venkatachalapathy V and Puttraj B 1985 *J. Mater. Sci.* **20** 1419
192. Boudjada A and Perret R 1975 *C. R. Acad. Sci. Paris* **C281** 31
193. Limaye S Y, Agrawal D K and McKinstry H A 1987 *J. Am. Ceram. Soc.* **70** C232
194. Yao P C and Fray D J 1983 *Solid State Ionics* **8** 35
195. Losilla E R, Aranda M A G, Bruque S, Sanz J, Paris M A, Campo J and West A R 2000 *Chem. Mater.* **12** 2134
196. Masquelier C, Wurm C, Rodriguez-Carvajal J, Gaubicher J and Nazar L 2000 *Chem. Mater.* **12** 525
197. Yoldas B E 1977 *J. Mater. Sci.* **12** 1203
198. Sakka S and Kamiya K 1980 *J. Non-Cryst. Solids* **42** 403
199. Mazdiyansni K S 1982 *Ceram. Int.* **8** 42
200. Lejeune M, Colomban Ph and Boilot J P 1982 *J. Non-Cryst. Solids* **51** 273
201. Susman S, Celbecq C J, Mc Millan J A and Roche M F 1983 *Solid State Ionics* **9&10** 667
202. Boilot J P and Colomban Ph 1985 *J. Mater. Sci. Lett.* **4** 22
203. Boilot J P, Colomban Ph and Collin G 1986 *Solid State Ionics* **18/19** 974
204. Colomban Ph 1986 *J. Mol. Struct.* **143** 191
205. Colomban Ph 1986 *Solid State Ionics* **21** 97
206. Sobha K C and Rao K J 1995 *Solid State Ionics* **81** 145
207. Sobha K C and Rao K J 1996 *J. Phys. Chem. Solids* **57** 1263
208. Sobha K C and Rao K J 1996 *J. Solid State Chem.* **121** 197
209. Alamo J 1993 *Solid State Ionics* **63–65** 547
210. Boilot J P, Salanié J P, Desplanches G and Le Potier D 1979 *Mater. Res. Bull.* **14** 1469
211. Alamo J 1993 *Solid State Ionics* **63–65** 678
212. Shanmugham S, More K L, Stinton D P, Hubbard C R, Cavin O B, Porter W D, Henson T J and Limaye S Y 1995 *Scr. Metall. Mater.* **32** 1967
213. Agrawal D K and Stubican V S 1985 *Mater. Res. Bull.* **20** 99
214. Padma Kumar P and Yashonath S 2002 *J. Am. Chem. Soc.* (*Commun.*) **124** 3828
215. Padma Kumar P and Yashonath S 2002 *J. Phys. Chem.* **B106** 7081
216. Boilot J G, Collin G and Colomban Ph 1988 *J. Solid State Chem.* **73** 160
217. Padma Kumar P and Yashonath S 2001 *J. Phys. Chem.* **B105** 6785
218. Padma Kumar P and Yashonath S 2002 *J. Phys. Chem.* **B106** 3443